Dynamic association of RNA-editing enzymes with the nucleolus

Joana M. P. Desterro[1], Liam P. Keegan[2], Miguel Lafarga[3], Maria Teresa Berciano[3], Mary O'Connell[2] and Maria Carmo-Fonseca[1,*]

[1]Institute of Molecular Medicine, Faculty of Medicine, University of Lisbon, 1649-028 Lisbon, Portugal
[2]MRC Human Genetics Unit, Western General Hospital, Crewe Road, Edinburgh, EH4 2XU, UK
[3]Department of Anatomy and Cell Biology, Biomedicine Unit Associated with the CSIC, University of Cantabria, Santander, Spain
*Author for correspondence (e-mail: carmo.fonseca@fm.ul.pt)

Accepted 15 January 2003
Journal of Cell Science 116, 1805-1818 © 2003 The Company of Biologists Ltd
doi:10.1242/jcs.00371

Summary

ADAR1 and ADAR2 are editing enzymes that deaminate adenosine to inosine in long double stranded RNA duplexes and specific pre-mRNA transcripts. Here, we show that full-length and N-terminally truncated forms of ADAR1 are simultaneously expressed in HeLa and COS7 cells owing to the usage of alternative starting methionines. Because the N-terminus of ADAR1 contains a nuclear export signal, the full-length protein localizes predominantly in the cytoplasm, whereas the N-terminally truncated forms are exclusively nuclear and accumulate in the nucleolus. ADAR2, which lacks a region homologous to the N-terminal domain of ADAR1, localizes exclusively to the nucleus and similarly accumulates in the nucleolus. Within the nucleolus, ADAR1 and ADAR2 co-localize in a novel compartment. Photobleaching experiments demonstrate that, in live cells, ADAR1 and ADAR2 are in constant flux in and out of the nucleolus. When cells express the editing-competent glutamate receptor *GluR-B* RNA, endogenous ADAR1 and ADAR2 de-localize from the nucleolus and accumulate at sites where the substrate transcripts accumulate. This suggests that ADAR1 and ADAR2 are constantly moving through the nucleolus and might be recruited onto specific editing substrates present elsewhere in the cell.

Key words: RNA editing, ADAR1, ADAR2, Nucleolus

Introduction

Conversion of adenosine to inosine within RNA drastically alters the base-pairing ability of the RNA and introduces diversity. In mRNA, inosine is translated as if it were guanosine (Basilio et al., 1962), whereas, in tRNA, inosine at position 34 or 37 influences base-pairing at the anticodon loop (for a review, see Keller et al., 1999). The adenosine deaminase acting on RNA (ADAR) family of enzymes convert adenosine to inosine in mRNA, whereas the adenosine deaminase acting on tRNA (ADAT) family deaminate adenosine to inosine in tRNA.

ADAR activity has been found in all metazoan species that have been examined. In mammals, there are three members of the ADAR family: ADAR1 and ADAR2 convert specific adenosine to inosine in pre-mRNA and can also convert up to 40-50% of the adenosines in long synthetic duplex RNAs (for a review, see Keegan et al., 2001). To date, no enzymatic activity has been detected for ADAR3 (Chen et al., 2000). ADAR1 and ADAR2 are expressed in most tissues but the pre-mRNAs that have been identified that are edited generally encode receptors of the central nervous system (for a review, see Emeson and Singh, 2000). These transcripts include the glutamate-gated ion channel receptors (GluR), the serotonin-2C receptor as well as a transcript encoding ADAR2 itself. Editing of transcripts can dramatically alter the properties of the receptor, for example editing of the Q/R site in GluR-B results in a glutamine codon being converted to an arginine codon, thereby generating a receptor impermeable to calcium ions (Sommer et al., 1991). Viral transcripts are also edited and these include transcripts of the hepatitis delta virus (Taylor, 1990) and DNA virus transcripts such as those of polyoma virus (Kumar and Carmichael, 1997). Highly edited transcripts of the polyoma virus accumulate in the nucleus and are not exported (Zhang and Carmichael, 2001). A sequence specific endonuclease that cleaves inosines in hyperedited RNA has been identified in the cytoplasm (Scadden and Smith, 2001). This endonuclease might be a means for the removal of hyper-edited viral RNA.

Because ADAR1 and ADAR2 are very similar, they display overlapping specificities at some editing sites, such as the GluR-B R/G site (Melcher et al., 1996; O'Connell et al., 1997). At other sites, there is an absolute requirement for one enzyme that cannot be compensated by the presence of the other. This was observed when transgenic mice were generated lacking ADAR2 and when heterozygote chimeras were generated for ADAR1 (Higuchi et al., 2000; Wang et al., 2000). The presence of the other active enzyme in the transgenic mice could not rescue the observed phenotype.

ADAT1 converts adenosine to inosine at position 37 that is beside the anticodon loop and is not essential in yeast (Gerber et al., 1998). Both ADARs and ADATs are members of the family of cytosine deaminases (CDAs), containing a deaminase domain with three distinctive motifs (Gerber and Keller, 2001). The amino acid residues in these motifs are thought to chelate a zinc ion at their active site. It has been proposed that the ADAR family evolved from the ADAT family, which have similar deaminase domain, and that they acquired double-

stranded RNA (dsRNA) binding domains (dsRBDs) to bind to pre-mRNA (Gerber et al., 1998). The residues in ADATs involved in binding to tRNA have not yet been identified. ADAT1 is more similar to the ADARs than ADAT2/3 (Gerber and Keller, 1999).

ADAR1 has three dsRBDs, whereas ADAR2 has two at the N-terminus (for a review, see Hough and Bass, 2000). ADAR1 differs from ADAR2 in that it has an extended N-terminus enriched in RG residues and contains two tandemly arranged Z-DNA-binding domains (ZBDs). Alternative splicing of transcripts from constitutively active promoters results in translation beginning at methionine 296 to produce a protein of 110 kDa (George and Samuel, 1999b; Kawakubo and Samuel, 2000). Transcripts from an upstream interferon-inducible promoter include a new exon 1A that contains a start codon and encodes a larger protein of 150 kDa. The 150 kDa protein is observed in the cytoplasm and is involved in the antiviral pathway, whereas the 110 kDa protein is present in the nucleus. Recently, a nuclear localization signal (NLS) has been described for ADAR1 that overlaps with the third dsRBD (Eckmann et al., 2001), whereas an nuclear export signal (NES) has been identified at the N-terminus at residue 127 (Poulsen et al., 2001).

Here, we report a systematic analysis of the intracellular localization of adenosine deaminase enzymes. Our results indicate that ADAR1 and ADAR2 are in a dynamic flux in and out of the nucleolus in the living cell. Transient sequestration of ADAR1 and ADAR2 in the nucleolus might be mediated by binding to the abundant dsRNA structures associated with small nucleolar RNAs, because the ADAR-related deaminase ADAT1, which lacks dsRBDs, fails to accumulate in this compartment.

Materials and Methods

Antibodies

Endogenous adenosine deaminase enzymes were detected using rabbit polyclonal antibodies raised against different regions of human ADAR1 (hADAR1) (anti-ADAR1: Ab 007 and Ab 668) and hADAR2 proteins (anti-ADAR2: Ab 70) (O'Connell et al., 1997).

FLAG-tagged constructs were detected using a polyclonal rabbit antibody anti-FLAG (oct A) (Santa Cruz Biotechnology). His-tagged constructs were detected using an anti-His monoclonal antibody (Qiagen). Green fluorescent protein (GFP) was detected with a mixture of two mouse monoclonal antibodies (anti-GFP clones 7.1 and 13.1) (Boehringer Mannheim). Goat polyclonal antibody C-19 (Santa Cruz Biotechnology) recognizes B23 nucleolar phosphoprotein. Additionally, the following antibodies were used: monoclonal antibody anti-fibrillarin 72B9 (Reimer et al., 1987); monoclonal antibodies 4F4 and 9H10 directed against hnRNP C and A, respectively (Burd and Dreyfuss, 1994; Choi and Dreyfuss, 1984); and monoclonal antibody anti-histone (clone H11-4, Roche).

Mammalian expression constructs

The polylinker of pSK (O'Connell et al., 1998) contains a unique *Eco*RI restriction site and into this site an epitope-tagged cassette was inserted that encoded an N-terminal FLAG epitope, a *Spe*I restriction site and a C-terminal histidine hexamer. Full-length hADAR1 and hADAR1C-Term (residues 443-1226) were subcloned into this expression vector via the *Spe*I restriction site to generate FLAG and histidine epitope-tagged versions, Flis-ADAR1 and Flis-ADAR1C-Term (O'Connell et al., 1995). Subsequently full-length hADAR1 and hADAR1C-Term were excised using the *Spe*I restriction site and inserted into the *Xba*I restriction site in pEGFP-C3 (Clontech), GFP-ADAR1 and GFP-ADAR1C-Term. To generate GFP-ADAR1N-Term, ADAR1N-Term (amino acids 1-442) was amplified by PCR with primers containing *Spe*I restriction sites and again inserted into the *Xba*I restriction site in pEGFP-C3. To generate GFP-ADAR2 and FlisADAR2, full-length hADAR2 was subcloned into the *Xba*I restriction site in pEGFP-C3 vector and into the *Spe*I restriction site of the FLAG and histidine epitope tagged vector previously described (Gerber et al., 1997). Flis-ADAR1 M296A mutant was generated using the QuickChange kit (Stratagene) and the following primers: 5′-GAGTTTTTAGACGCGGCCGAGATCAAG-3′, 5′-CTTGATCT-CGGCCGCGTCTAAAAACTC-3′.

GFP-ADAR2 deletions, Δ64-75, Δ64-132 were performed using ExSite™ PCR-Based Site-Directed Mutagenesis Kit (Stratagene), GFPADAR2 as template and the following primers: 5′-GGAGTG-GCCATTGCTGCCCTCCTCCAG-3′, 5′-CCCGTCCTCCCCAAG-AACGCCCTGATG-3′ and 5′-CATGCTGCTGAGAAGGCCTTG-AGGTC-3′. GFP-ADAR2 ΔN was obtained by digestion of GFP-ADAR2 WT with *Stu*I restriction enzyme and cloned into pEGFP-C3 vector digested with *Stu*I and *Sma*I. GFP-N1-ADAR2 was excised from GFP-ADAR2 WT using *Eco*RI and *Stu*I restriction sites and inserted into pEGFP-C3 vector digested with *Eco*RI and *Sma*I.

Full-length human hADAT1 was amplified by PCR from a human fetal brain cDNA library (Keegan et al., 2000) and inserted in the pEGFP-C3 vector at the *Xba*I restriction site to generate GFP-ADAT. All constructs were confirmed by sequencing.

Cell culture, heterokaryon assays and drugs treatment

Human HeLa, COS7 and murine NIH 3T3 cells were cultured as monolayers in Modified Eagle's Medium (MEM) and Dulbecco's Modified Eagle's Medium (DME), respectively (Gibco-BRL, Paisley, Scotland). All media were supplemented with 10% fetal calf serum (FCS, Gibco-BRL). Heterokaryons were obtained as previously described (Calado et al., 2000). Briefly, 1.5×10^6 3T3 cells were plated over subconfluent HeLa cells grown on coverslips on 35×10 mm tissue culture dishes. 3T3 cells were allowed to adhere for 3 hours at 37°C, 5% CO_2, in the presence of 20 μg ml^{-1} emetine. The cells were then placed in complete MEM medium with 20 μg ml^{-1} emetine and incubated for further 3 hours. To induce cell fusion, coverslips were rinsed in PBS and placed on a drop of polyethylene-glycol (PEG 1500; Roche Biochemicals, Indianapolis, IN, USA) for 2 minutes. The coverslips were then washed in PBS and further incubated in culture medium at 37°C for 4 hours.

To induce segregation of the different nucleolar component, actinomycin D (Sigma) was added to the tissue culture medium at a final concentration of 0.07 μg ml^{-1} 1 hour before fixation. To inhibit nuclear export, leptomycin B (LMB; Sigma) was added at a final concentration of 50 nM to the tissue culture medium 3 hours before fixation.

Transfections

Mainly HeLa cells but also COS7 cells were used for transfections studies. DNA for transfection assays was purified using the Qiagen plasmid DNA midi-prep kit (Qiagen, Hilden, Germany). HeLa subconfluent cells grown on glass coverslips in 35×10 mm tissue culture dishes were transiently transfected with 1 μg of purified plasmid DNA and using FuGene6 Reagent (Roche Biochemicals, Indianapolis, IN, USA) according to the manufacturer's protocol. Subconfluent COS7 cells seeded in 25 cm^3 flasks were transiently transfected with purified plasmid DNA by mixing with Lipofectamine (Gibco BRL) according to the manufacturer's protocol. Cells were analyzed at 16-24 hours after transfection.

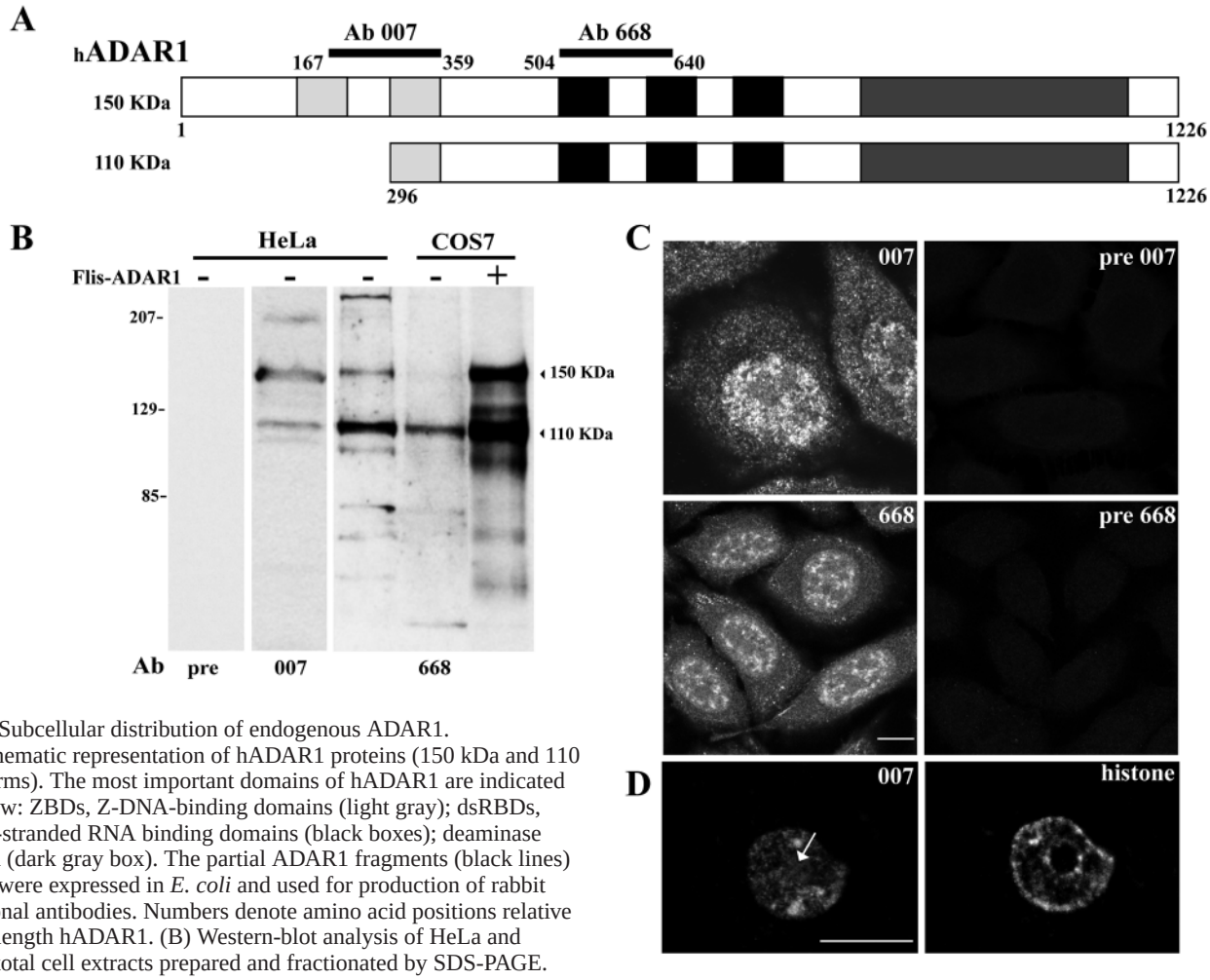

Fig. 1. Subcellular distribution of endogenous ADAR1. (A) Schematic representation of hADAR1 proteins (150 kDa and 110 kDa forms). The most important domains of hADAR1 are indicated as follow: ZBDs, Z-DNA-binding domains (light gray); dsRBDs, double-stranded RNA binding domains (black boxes); deaminase domain (dark gray box). The partial ADAR1 fragments (black lines) shown were expressed in *E. coli* and used for production of rabbit polyclonal antibodies. Numbers denote amino acid positions relative to full-length hADAR1. (B) Western-blot analysis of HeLa and COS7 total cell extracts prepared and fractionated by SDS-PAGE. Western blotting was then performed with a pre-immune serum (lane 1) and with anti-ADAR1 antibodies: 007 (lane 2) and 668 (lane 3-5). Extracts of COS7 cells transiently transfected with Flis-ADAR1 (Fig. 2) are shown in lane 5. All antibodies recognized the full-length hADAR1 (150 kDa) and the 110 kDa form of ADAR1. Molecular weight markers are shown on the left. (C) HeLa cells were immunostained with antibodies 007 and 668, and with the respective pre-immune sera. The panels are representative of the labeling patterns observed. (D) Neurosecretory neurons from the supraoptic nucleus were obtained from squash preparations of rat hypothalamus and analysed by indirect immunofluorescence. The cells were double-labeled with affinity-purified anti-ADAR1 antibody (007) and an anti-histone antibody. The ADAR1 antibody produces a non-homogeneous nucleoplasmic staining, with additional labeling of the nucleolus (arrow). Within the nucleoplasm, the antibody decorates nuclear speckles. Bar, 10 μm.

Western blotting

Western-blot analysis of transfected cells was performed for all constructs as previously described (Gama-Carvalho et al., 1997) using whole-cell extracts that were prepared in SDS sample buffer. Lysates were boiled for 10 minutes prior to fractionation by electrophoresis in either 10% or 12.5% polyacrylamide gels and transferred to a PVDF membrane by electroblotting. Anti-His, anti-GFP and anti-FLAG were used as primary antibodies. Horseradish peroxidase-conjugated anti-mouse IgG and anti-rabbit IgG (Amersham) were used as secondary antibodies. Blots were developed with an enhanced chemiluminescence detection system.

Immunofluorescence and immunoelectron microscopy

Cells on coverslips were briefly rinsed in PBS, fixed in 3.7% formaldehyde (freshly prepared from paraformaldehyde), diluted in PBS for 10 minutes at room temperature and washed in PBS. The cells were then permeabilized with either 0.5% Triton X-100 for 15 minutes or 0.05% SDS for 10 minutes at room temperature and washed in PBS. Immunofluorescence and confocal microscopy were performed as described (Calado et al., 2000). For analysis of hypothalamic neurons, supraoptic nuclei were dissected out of male 3-month-old rats of the Sprague-Dawley strain. Immunofluorescence and immunoelectron microscopy of tissue samples were performed as described (Lafarga et al., 1998).

In situ hybridization

GluR-B DNA was obtained by *Sma*I and *Xba*I digestion of the GluR-B/pRK plasmid (Higuchi et al., 1993). This fragment and the plasmid containing the C-RNA were purified, labeled with digoxigenin –11-dUTP by nick translation (Lichter et al., 1991) and used as probes for in situ hybridization. Before in situ hybridization, cells were immunostained as described with the required antibody and fixed for 10 minutes in 1% formaldehyde. Fixed cells were then washed with PBS and, immediately before hybridization, were incubated in hybridization mixture for 5 minutes at 37°C. Cells were hybridized for 4 hours at 37°C in 50% formamide, 2× SSC, 10% dextran sulfate,

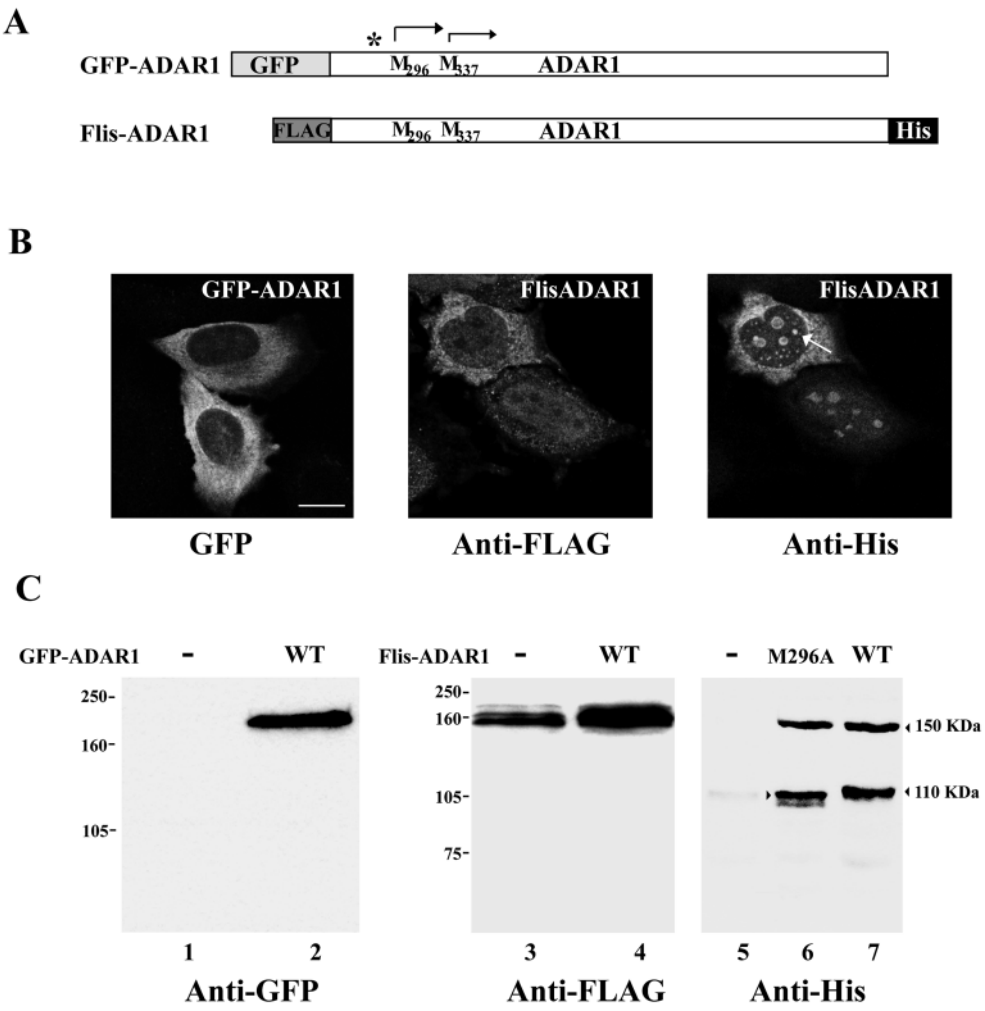

Fig. 2. The full-length (150 kDa) form of hADAR1 localizes to the cytoplasm and the short (110 kDa) form localizes to the nucleolus. (A) Schematic representation of differently tagged hADAR1 constructs. In-frame methionines present in hADAR1 cDNA are shown (M296, M337). The NLS recently described by Eckmann et al. (Eckmann et al., 2001) is marked by an asterisk (*). (B) HeLa cells were transiently transfected with the indicated hADAR1 constructs and assayed for ADAR1 localization by either direct detection of GFP or indirect immunofluorescence using anti-FLAG and anti-His antibodies. GFP- and FLAG-tagged ADAR1 localize to the cytoplasm. The anti-His antibody stains both the cytoplasm and the nucleolus. In addition, the anti-His antibody labels discrete aggregates in the nucleoplasm (arrow). (C) Western-blot analysis of total proteins from COS7 cells transfected with the indicated plasmids. Total cell extracts after 36 hours of expression were prepared and fractionated by SDS-PAGE. Western blotting was then performed with an anti-GFP antibody (lanes 1, 2), an anti-FLAG antibody (lanes 3, 4) and an anti-His antibody (lanes 5-7). The western-blot signal observed with mobility just below that of the ADAR1 band with the anti-FLAG antibody is a nonspecific signal also present in non-transfected cells (Fig. 2C, lanes 3,4). Both antibodies recognize the full-length (150 kDa) hADAR1 but the short (110 kDa) form of the protein is only specifically detected with anti-His antibody. Molecular weight markers are shown on the left.

50 nM sodium phosphate pH 7.0 with probes at 2 ng μl^{-1}. Post-hybridization washes were in 50% formamide, 2× SSC (three times for 5 minutes at 45°C) and in 2× SSC (three times for 5 minutes at 45°C). The sites of hybridization were visualized using a cy3 anti-digoxigenin secondary antibody (Molecular Probes) diluted in 4× SSC-Tween, 2% bovine serum albumin, 0.2% gelatin.

FRAP and FLIP analysis

Live cells were imaged at 37°C maintained by a heating/cooling frame (LaCon, Germany) in conjunction with an objective heater (PeCon, Germany). Images were acquired on a Zeiss LSM 510 with the Planapochromat 63×/1.4 objective. Enhanced green fluorescence protein (EGFP) fluorescence was detected using the 488 nm laser line of an argon laser (25 mW nominal output) in conjunction with a LP 505 filter. Each FRAP (fluorescence recovery after photobleaching) analysis started with three image scans, followed by a bleach pulse of 0.5 seconds on a spot with the size of a nucleolus. Single section images were collected at 3 second intervals. For imaging, the laser power was attenuated to 0.1-0.2% of the bleach intensity. The average fluorescence in the nucleus $T(t)$ and the average fluorescence in the bleached region $I(t)$ were calculated for each background subtracted image at time t after bleaching. FRAP recovery curves were normalized according to Phair and Misteli (Phair and Misteli, 2000).

$$Irel(t) = \frac{I(t)}{I_i}\,\frac{T_i}{T(t)}\,,$$

where T_i is the fluorescence in the nucleus before bleaching and I_i is the fluorescence in the bleached region before bleaching. This normalization corrects for the loss of fluorescence caused by imaging. Typically, ~10% of the total EGFP fluorescence was lost during the bleach pulse. During the post-bleaching scanning phase, the fluorescence lost was <5% for EGFP.

For FLIP (fluorescence loss in photobleaching) experiments, cells were repeatedly bleached at intervals of 4.5 seconds and imaged between bleach pulses. Bleaching was performed by 538-millisecond bleach pulses on a spot with a diameter equivalent to that of a nucleolus. Repetitive bleach pulses were achieved, taking advantage of the trigger interface for LSM 510. An electronic oscillator circuit was built to create pulses with a user-defined frequency. When connected to the LSM 510, it would then trigger the bleaching events. A series of 600 images were collected for each cell with laser power attenuated to 1% of the bleach intensity. Nuclear fluorescence of selected areas in FLIP experiments was measured using the ROI mean function of the LSM 510 Physiology Package. The data were then background subtracted and normalized to correct loss of fluorescence caused by imaging, in a similar way to FRAP but using an adjacent cell to estimate $T(t)$ and T_0. Loss of fluorescence caused by imaging could reach 20-25% over the time course of the experiment.

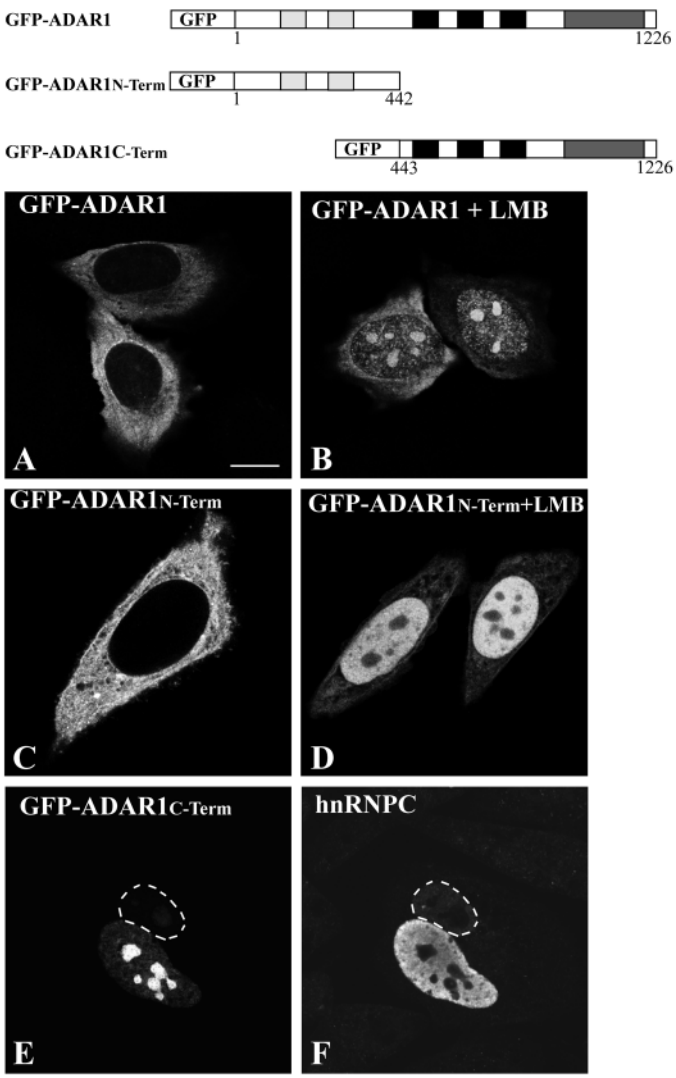

Fig. 3. hADAR1 shuttles between the cytoplasm and the nucleus and localizes to the nucleolus with no requirement for the N-terminal domain. N-terminal and C-terminal deletions of hADAR1 were fused to GFP. The most important domains of hADAR1 are indicated as follow: ZBDs, Z-DNA-binding domains (light gray); dsRBDs, double-stranded RNA binding domains (black boxes); deaminase domain (dark gray box). Numbers denote amino-acid positions relative to the N-terminus of hADAR1. HeLa cells were transfected with the indicated constructs and, approximately 18 hours after transfection, the cells were incubated with or without 50 nM LMB for 3 hours, fixed and observed directly with the fluorescence microscope. Notice that the cytoplasmic chimera resulting from the C-terminal deletion (C) accumulates in the nucleus with nucleolar exclusion after LMB treatment (D), whereas the full-length fusion protein (A) is concentrated in the nucleolus after LMB treatment (B). HeLa cells transfected with GFP-ADAR1C-Term were fused with murine 3T3 cells to form heterokaryons. These cells were treated with a protein synthesis inhibitor (emetine, 20 μg ml^{-1}) for 3 hours before fusion. After fusion, the cells were kept in culture for 3 hours in the presence of emetine. Heterokaryons were fixed and labeled with monoclonal antibody 4F4 directed against hnRNP C protein, which does not shuttle. Like hnRNP C (F), the N-terminal deletion of hADAR1 remains restricted to the transfected HeLa cell nucleus (E). The dashed lines in E and F indicate the contour of the murine nucleus in the heterokaryon. Notice that the N-terminal deletion of ADAR1 localizes exclusively to nucleoli (E). Bar, 10 μm.

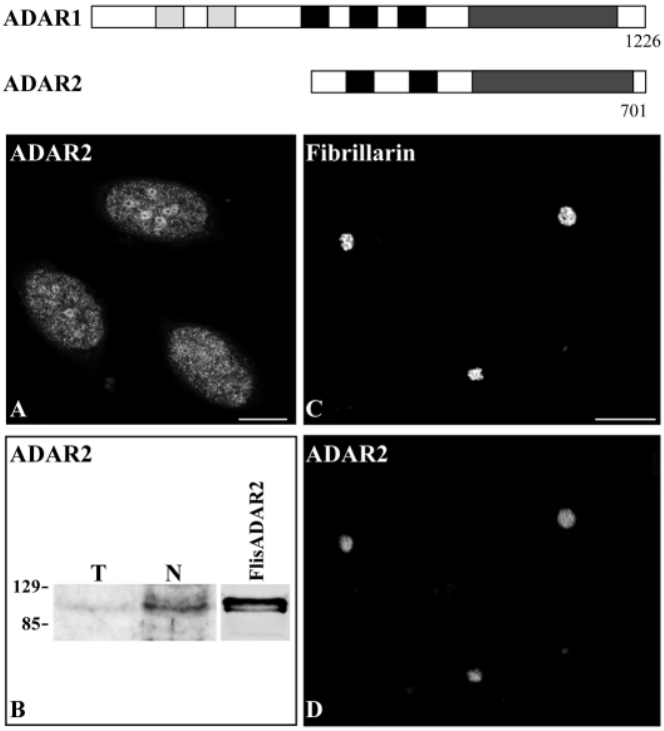

Fig. 4. Subcellular distribution of endogenous ADAR2. Schematic diagram comparing hADAR1 and hADAR2. The numbers indicated at the C-terminus represent size of the protein in amino acids. The most important domains of hADAR1 are indicated as follow: ZBDs, Z-DNA-binding domains (light gray); dsRBDs, double-stranded RNA binding domains (black boxes); deaminase domain (dark gray box). (A) HeLa cells were immunolabeled with anti-ADAR2 antibody. The labeling pattern is diffuse throughout the nucleoplasm, with concentration in nucleoli. The relative concentration of ADAR2 staining in the nucleolus varies from cell to cell. (B) A western-blot analysis of total (T) and nuclear (N) HeLa cell extracts. Cell extracts were prepared and fractionated by SDS-PAGE. Western blotting was then performed with anti-ADAR2 antibody (Ab 70). Extracts of HeLa cells transiently transfected with FlisADAR2 are shown in lane 3. Molecular weight markers are shown on the left.
(C,D) Cryosections of neurosecretory neurons from the hypothalamic supraoptic nucleus were double-labeled with antibodies directed against fibrillarin (C) and ADAR2 (D). ADAR2 is predominantly detected in nucleoli, which can be readily identified by the fibrillarin staining. Bar, 10 μm.

Results

hADAR1 localizes in the cytoplasm, nucleoplasm and nucleoli

ADAR1 is ubiquitously expressed and previous observations indicated that there are two forms of this enzyme in humans: a 150 kDa protein (comprising amino acids 1-1226) that is induced by interferon and localizes predominantly in the cytoplasm, and a 110 kDa protein (encompassing residues 296-1226) that is constitutively expressed and localizes to the nucleus (George and Samuel, 1999a; George and Samuel, 1999b; Patterson and Samuel, 1995). To further characterize the subcellular distribution of the ADAR1 enzyme, indirect immunofluorescence microscopy was performed using rabbit polyclonal antibodies raised against fragments of the human

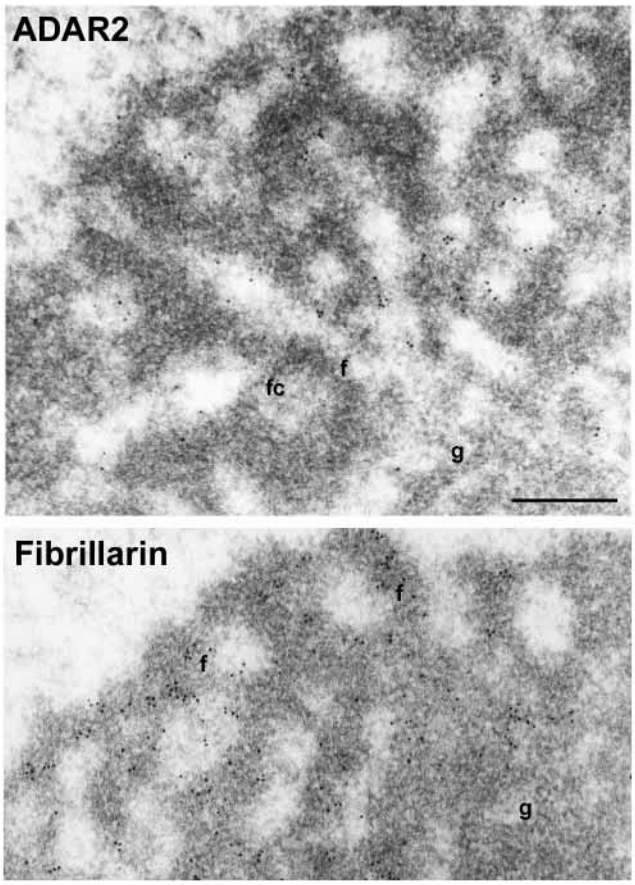

Fig. 5. Electron microscopy reveals that ADAR2 localizes in a novel subnucleolar compartment. Ultrathin sections from rat brain neurons were immunogold labeled with antibodies directed against ADAR2 and fibrillarin. The ADAR2-specific gold particles decorate the periphery of the fibrillar component (f) and are largely excluded from the fibrillar centers (fc) and the granular component (g). By contrast, the anti-fibrillarin antibody produces an intense labeling of the dense fibrillar component. Bar, 300 nm.

protein (hADAR1) expressed in *Escherichia coli*. A schematic representation of hADAR1 forms and the different segments used for production of antibodies is shown in Fig. 1A. Ab 007 was raised against the region encompassing amino acids 167-359, which corresponds to the ZBDs, and Ab 668 was raised against the first two dsRBDs (amino acids 504-640). Western-blot analysis of HeLa and COS7 total cell extracts shows that both antibodies recognize two polypeptides of 150 kDa and 110 kDa (Fig. 1B, lanes 2-4), whereas the pre-immune serum is devoid of any reactivity (Fig. 1B, lane 1). For comparison, COS7 cells were transiently transfected with a plasmid containing the full-length hADAR1 cDNA tagged with both a Flag epitope and a histidine hexamer (Flis-ADAR1; Fig. 2). Total protein extracts from the transfected cells were probed with Ab 668 and the results confirm that the 150 kDa and 110 kDa protein bands correspond to the long and short forms of hADAR1 (Fig. 1B, lane 5).

Immunofluorescence analysis of HeLa cells incubated with antibodies 007 and 668 reveals predominant labeling of the cell nucleus with additional staining of the cytoplasm (Fig. 1C). Within the nucleus, there is an intense nucleoplasmic staining with additional, albeit weaker, labeling of nucleoli. The nucleoplasmic labeling is not homogeneous, with a higher concentration in nuclear speckles, as confirmed by double-labeling experiments using antibodies directed against spliceosome components (data not shown). The intensity of nucleolar staining varies from cell to cell. Similar immunofluorescence results were observed in HeLa and COS7 cells (data not shown).

Because most of the known ADAR-edited transcripts in mammals are expressed in the central nervous system (Gott and Emeson, 2000; Palladino et al., 2000; Patton et al., 1997), we decided to examine the distribution pattern of ADAR1 in sections of rat brain. Consistent with the data observed in cultured cell lines, the Ab 007 labels predominantly the nucleus of hypothalamic neurons (Fig. 1D). Although the labeling is more prominent in the nucleoplasm, the antibody also stains the nucleolus (Fig. 1D, arrow). Thus, ADAR1 appears to be distributed throughout the cytoplasm and the nucleus, including the nucleolus.

To verify the localization of endogenous ADAR1 observed by immunofluorescence, we next analysed the distribution of tagged versions of ADAR1. Two different constructs were generated using the full-length hADAR1 cDNA. One construct encodes hADAR1 tagged with GFP at the N-terminus (GFP-ADAR1). The other encodes hADAR1 tagged simultaneously with a N-terminal Flag epitope and a C-terminal histidine hexamer (Flis-ADAR1) (Fig. 2A).

When HeLa cells were transfected with GFP-ADAR1 and directly observed in the fluorescence microscope, the labeling was exclusively detected in the cytoplasm (Fig. 2B). Western-blot analysis of total protein extracts from untransfected and transfected cells probed with anti-GFP antibodies (Fig. 2C, lanes 1, 2) shows a single band of ~180 kDa, which corresponds to the expected molecular weight of the full-length ADAR1 (150 kDa) fused to GFP (27 kDa). The localization of full-length ADAR1 to the cytoplasm is consistent with the presence of a nuclear export signal (NES) at the N-terminus of the protein (amino acids 125-137) (Eckmann et al., 2001).

Next, HeLa and COS7 cells were transfected with Flis-ADAR1 and probed with anti-Flag and anti-His antibodies. By western blot, the anti-Flag antibody reacts with the full-length form of ADAR1 (Fig. 2C, lane 4), whereas the anti-His antibody reveals both the full-length (150 kDa) and the shorter (110 kDa) forms of the protein (Fig. 2C, lane 7). The same two protein bands are detected when total protein extracts from cells transfected with Flis-ADAR1 are probed with anti-ADAR1 antibody (Fig. 1B, lane 5). The shorter form of ADAR1 was previously suggested to result from a proteolytic cleavage of the N-terminus of the full-length protein (Patterson and Samuel, 1995). Nevertheless, the presence of an in-frame methionine precisely at residue 296 raises the possibility of alternative starting sites being used by the translation machinery. Because ADAR1 contains a further in-frame methionine at residue 337, we generated a Flag/His tagged hADAR1 construct with methionine 296 mutated to an alanine (M296A). When this construct was transfected into either HeLa or COS7 cells, a protein band with slightly higher mobility was observed by western blotting with the anti-His antibody (Fig. 2C, lane 6, arrowhead). The appearance of this shorter protein product corresponding to a polypeptide starting at methionine 337 supports the view that synthesis of the 150 kDa and 110 kDa forms of ADAR1 can be caused by

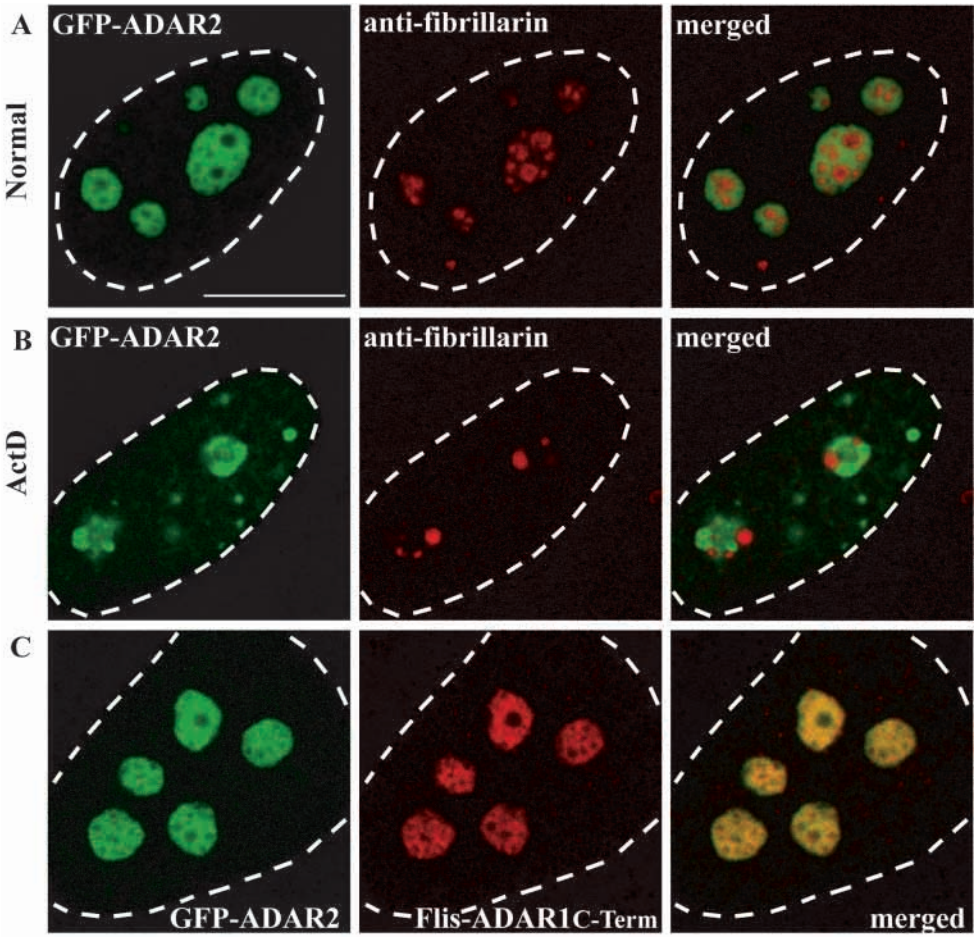

Fig. 6. hADAR1 and hADAR2 co-localize within the nucleolus. HeLa cells were transfected with GFP-ADAR2, incubated in the absence (A) or in the presence (B) of actinomycin D (0.07 μg ml^{-1}) for 1 hour and double-labeled with a monoclonal antibody against fibrillarin. The merged images show clearly that GFP-ADAR2 (green) and fibrillarin (red) do not co-localize. (C) HeLa cells were co-transfected with GFP-ADAR2 and Flis-ADAR1C-Term (Fig. 2A). Approximately 16 hours after transfection, cells were fixed, immunostained with anti-FLAG antibody (red) and analysed by confocal microscopy. GFP-ADAR2 and Flis-ADAR1 co-localize in the nucleolus of co-transfected cells, as can be seen in the merged image (yellow). Images from the same microscopic fields are shown side by side. The dashed lines indicate the contour of the HeLa cell nucleus. Bar, 10 μm.

alternative usage of either M_1 or M_{296} as starting methionines. However, we cannot exclude the possibility that a proteolytic event is taking place in parallel.

When double-immunofluorescence experiments were performed on cells transfected with Flis-ADAR1, the anti-Flag antibody produced exclusive staining of the cytoplasm, whereas the anti-His antibody labeled both the cytoplasm and the nucleus, with prominent staining of nucleoli (Fig. 2B). Staining of the cytoplasm and nucleoli was similarly observed when cells transfected with Flis-ADAR1 were incubated with anti-ADAR1 antibody 668 (data not shown). These results suggest that anti-FLAG antibody detects exclusively the 150 kDa protein (which localizes to the cytoplasm), whereas anti-His antibody reacts with both the 150 kDa and the 110 kDa proteins (which localize to the nucleolus). Interestingly, overexpression of exogenous ADAR1 leads to the appearance of discrete aggregates in the nucleoplasm that are reminiscent of nuclear speckles (Fig. 2B arrow, and data not shown). However, double-labeling experiments using antibodies against splicing factors show that these structures are distinct from the nuclear speckles where spliceosomal components accumulate (data not shown).

In conclusion, the data show that endogenous hADAR1 in HeLa and COS7 cells is present in two distinct forms of 150 and 110 kDa. The same two proteins are produced by transient transfection of the full-length hADAR1 cDNA, presumably owing to alternative usage of starting methionines. The long form of ADAR1 enzyme localizes predominantly to the cytoplasm, whereas the short form is nuclear and accumulates in the nucleolus. The results obtained with epitope-tagged proteins are consistent with the immunofluorescence analysis that reveals the presence of endogenous ADAR1 in the cytoplasm, nucleoplasm and nucleolus.

The C-terminal region of hADAR1 targets it to the nucleolus

Recent studies have shown that hADAR1 shuttles between the nucleus and the cytoplasm and contains a CRM1-dependent nuclear export signal in its N-terminus (Poulsen et al., 2001). Although putative nuclear localization signals (NLSs) have been predicted by sequence analysis in the same region of the protein, these are not biologically active. Instead, an NLS that overlaps with the third dsRNA-binding domain is responsible for nuclear import of the protein (Eckmann et al., 2001). Our observation that both endogenous and transfected hADAR1 are present in the nucleolus leads us to investigate which domains of the protein are responsible for the nucleolar targeting.

First, we asked whether the full-length protein, which (at steady state) localizes predominantly to the cytoplasm but is constantly shuttling to the nucleus, can be targeted to the nucleolus. To address this question, HeLa cells were transfected with GFP-tagged full-length hADAR1 and treated with LMB, a specific inhibitor of the CRM1 export receptor.

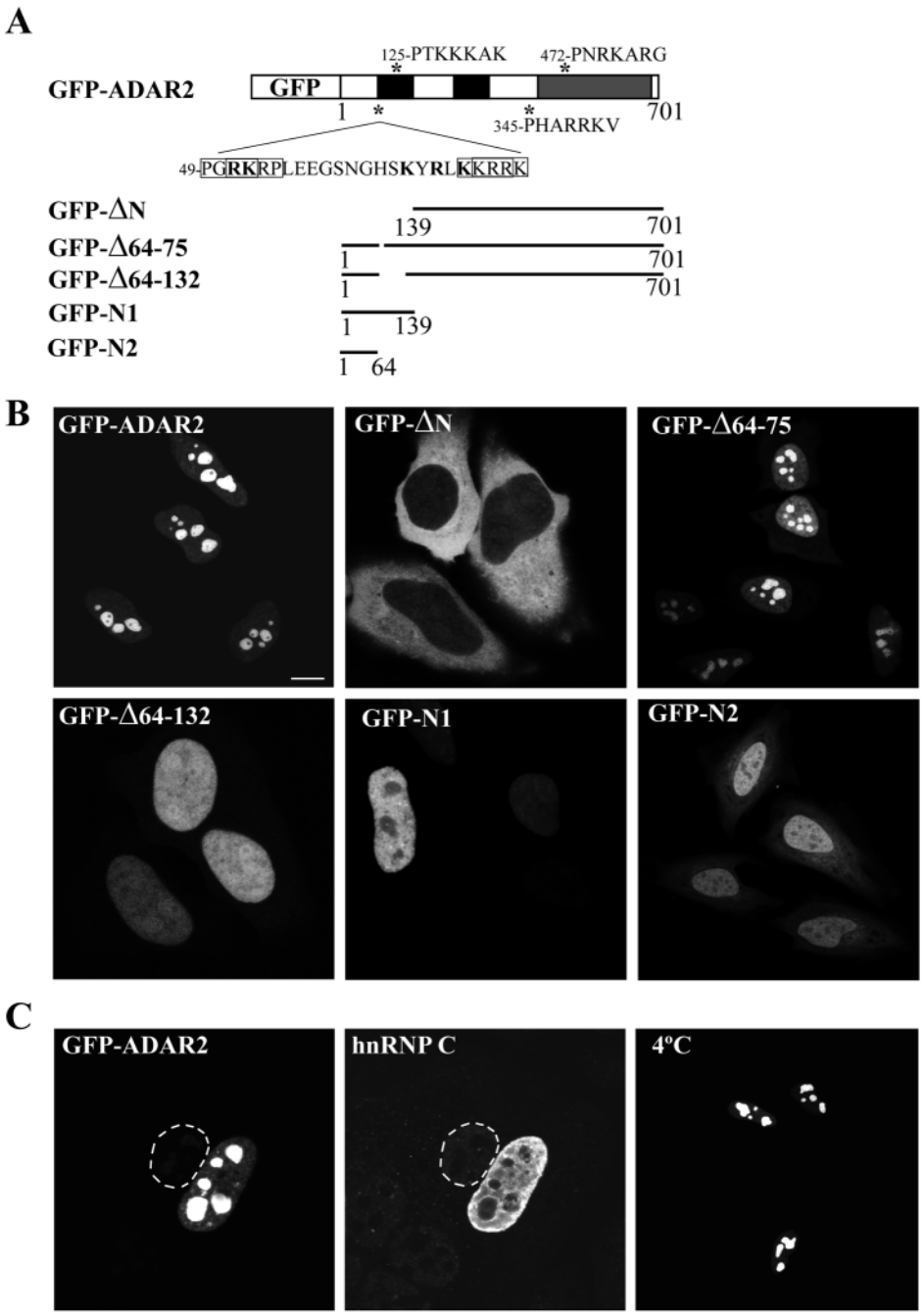

Fig. 7. hADAR2 does not shuttle and an N-terminal domain is responsible for its nuclear localization. (A) Schematic representation of the GFP-tagged full-length hADAR2 and the GFP-ADAR2 deletions constructed to study putative localization signals in hADAR2. Numbers denote amino acid positions relative to the N-terminus of hADAR2. Asterisks indicate putative NLSs identified by sequence analysis, and the respective amino acid sequences are shown. (B) HeLa cells were transiently transfected with the indicated GFP-ADAR2 constructs. Approximately 16 hours after transfection, cells were fixed and directly observed with the fluorescence microscope. (C) HeLa cells were transfected with GFP-ADAR2 and fused with murine NIH 3T3 cells. The heterokaryons were incubated in the presence of emetine. Immunostaining with anti-hnRNP C was used as control. Both GFP-ADAR2 and hnRNP C molecules remain restricted to the transfected HeLa nucleus. The dashed lines indicate the contour of the murine nucleus in the heterokaryon. Incubation of HeLa cells expressing GFP-ADAR2 at 4°C in the presence of emetine shows that the protein does not leak to the cytoplasm. Bar, 10 μm.

LMB treatment induced accumulation of GFP-hADAR1 in the nucleus as previously described (Eckmann et al., 2001; Poulsen et al., 2001), with clear concentration in nucleoli in most of the cells (Fig. 3A,B). Next, two GFP-tagged deletions of hADAR1 were constructed and their localization analysed. As expected, the GFP fusion with the N-terminal region of hADAR1 (GFP-ADAR1N-Term), which contains a functional NES (Poulsen et al., 2001), is exclusively detected in the cytoplasm (Fig. 3C). By contrast, the C-terminal region of hADAR1, which harbors a NLS in the third dsRBD, accumulates exclusively in nucleolus (Fig. 3E). When cells transfected with the N-terminal version of hADAR1 are treated with LMB, the protein accumulates in the nucleoplasm (Fig. 3D), indicating the presence of an additional functional NLS in the N-terminus as previously reported (Poulsen et al., 2001). This protein is completely excluded from the nucleolus, showing that the nucleolar targeting signal is contained in the C-terminal region of hADAR1.

Following the observation that the N-terminus of hADAR1 harbors an NLS, we asked whether an additional NES is present in the C-terminal region. An interspecies heterokaryon assay was therefore performed to determine whether GFP-ADAR1C-Term is a shuttling protein. The distribution of GFP-ADAR1C-Term was monitored in human-mouse heterokaryons produced by polyethylene-glycol-induced fusion of HeLa and murine NIH 3T3 cells (Calado et al., 2000). Heterokaryons were kept in culture for up to 6 hours in the presence of the protein-synthesis inhibitor emetine. As

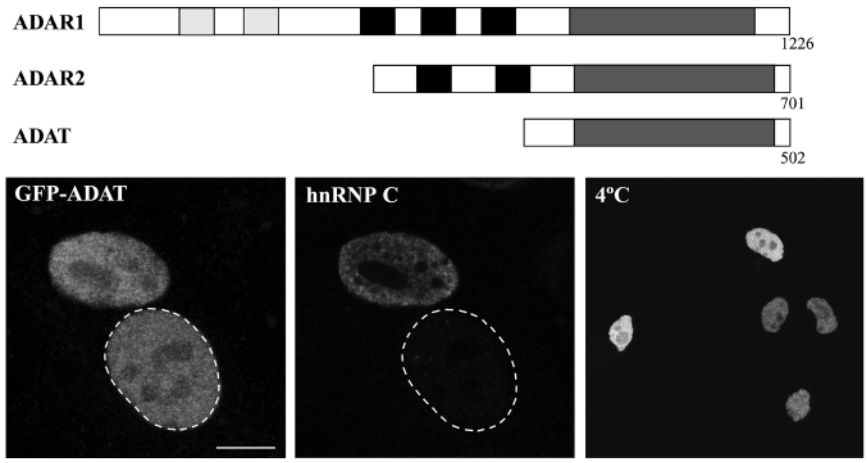

Fig. 8. hADAT1 is a nucleocytoplasmic shuttling protein that is excluded from the nucleolus. Schematic representation of the homology between hADAR1, hADAR2 and hADAT1. The three enzymes contain a deaminase domain and only hADAT1 does not contain dsRNA-binding domains. The most important domains of hADAR1 are indicated as follow: ZBDs, Z-DNA-binding domains (light gray); dsRBDs, double-stranded RNA binding domains (black boxes); deaminase domain (dark gray box). The size of the proteins are indicated at their C-termini as the number of amino acids. HeLa cells were transfected with GFP-ADAT1 and fused with murine NIH 3T3 cells. The heterokaryons were incubated in the presence of emetine. Immunostaining with anti-hnRNP C was used as control. In contrast to hnRNP C, which remains restricted to the transfected HeLa nucleus, GFP-ADAT1 migrates to the murine nuclei. The dashed lines indicate the contour of the murine nuclei in the heterokaryon. Incubation of HeLa cells expressing GFP-ADAT1 at 4°C in the presence of emetine shows that the protein does not leak to the cytoplasm. Bar, 10 μm.

controls, heterokaryons were labeled with monoclonal antibodies specific for human hnRNP C (a protein that does not shuttle) and hnRNP A (a protein that shuttles constantly between the nucleus and the cytoplasm) (Pinol-Roma and Dreyfuss, 1992). In the presence of emetine, both human hRNP C (Fig. 3F) and GFP-ADAR1C-Term (Fig. 3E) remain restricted to the human nucleus, demonstrating the inability of the hADAR1C-Term to shuttle. Under the same conditions, the shuttling protein hnRNP A was readily detected in the murine nucleus (data not shown).

In summary, these data confirm the presence of an NLS within the N-terminus of hADAR1, and show that the C-terminal region of the protein encompassing amino acids 443-1226 harbors a nucleolar targeting signal.

hADAR2 and hADAR1 co-localize within the nucleolus

Given the high homology between the C-terminal region of hADAR1 and human ADAR2 (hADAR2) (Fig. 4), we next analysed the cellular distribution of hADAR2. Indirect immunofluorescence was performed in HeLa cells using a specific anti-ADAR2 antibody (O'Connell et al., 1997). The results show that ADAR2 is nucleoplasmic and highly enriched in nucleoli in a large proportion of cells (Fig. 4A). Western-blot analysis confirms that the antibody reacts with a specific protein band in cells transfected with full-length ADAR2 cDNA (Fig. 4B, Flis-ADAR2). The results further reveal a very low abundance of endogenous ADAR2 in total HeLa cell extracts, with a significant concentration of the protein in the nuclear fraction (Fig. 4B).

Next, the anti-ADAR2 antibody was used to perform immunofluorescence in brain tissue, where the enzyme is expressed at higher level (Gerber et al., 1997). As shown in Fig. 4C,D, ADAR2 is predominantly localized to nucleoli of neurons from the hypothalamic supra-optic nucleus. To further characterize the subnucleolar localization of ADAR2, immunoelectron microscopy was performed on rat hypothalamic neurons. As shown in Fig. 5, the immunogold particles tend to cluster at the periphery of the dense fibrillar component, showing no obvious association with either fibrillar centers or granular regions. To extend these observations, HeLa cells were transfected with a plasmid encoding GFP-ADAR2 and immunostained with anti-fibrillarin antibody, which is a marker for the dense fibrillar component. Clearly, GFP-ADAR2 and fibrillarin do not co-localize in the nucleolus (Fig. 6A). The spatial separation between ADAR2 and fibrillarin is even more evident following treatment of cells with actinomycin D, which causes segregation of the different nucleolar components (Fig. 6B). Lack of co-localization was further observed between GFP-ADAR2 and markers for the fibrillar center and the granular component (data not shown).

Taken together, our results show that ADAR2 is localized to a specific subnucleolar compartment. This was confirmed by analysing the distribution of both endogenous ADAR2 in hypothalamic neurons (by electron microscopy) and GFP-tagged hADAR2 transiently expressed in HeLa cells.

Given that hADAR1 is also present in the nucleolus, we thought to compare the subnucleolar distribution of both editing enzymes. Treatment with LMB causes full-length GFP-ADAR1 to accumulate in the nucleolus (Fig. 3B), where it localizes with Flis-ADAR1C-Term (data not shown). We then co-transfected HeLa cells with GFP-ADAR2 and Flis-ADAR1C-Term. The staining of hADAR2 (Fig. 6C, green) and hADAR1C-Term (Fig. 6C, red) revealed almost identical patterns of nucleolar localization, as confirmed by merging the green and red images (Fig. 6C, merged). We therefore conclude that ADAR1 and ADAR2 localize to the same subnucleolar compartment.

Identification of hADAR2 nuclear and nucleolar localization signals

Having established that ADAR2 and the C-terminal region of ADAR1 are predominantly localized in nucleoli, we next compared the sequences of the two proteins. Sequence alignments of the hADAR1 NLS (Eckmann et al., 2001) with human and rat ADAR2 enzymes revealed that this region is not conserved (data not shown). Sequence analyses of hADAR2 yielded various putative NLSs in the N-terminus of the protein

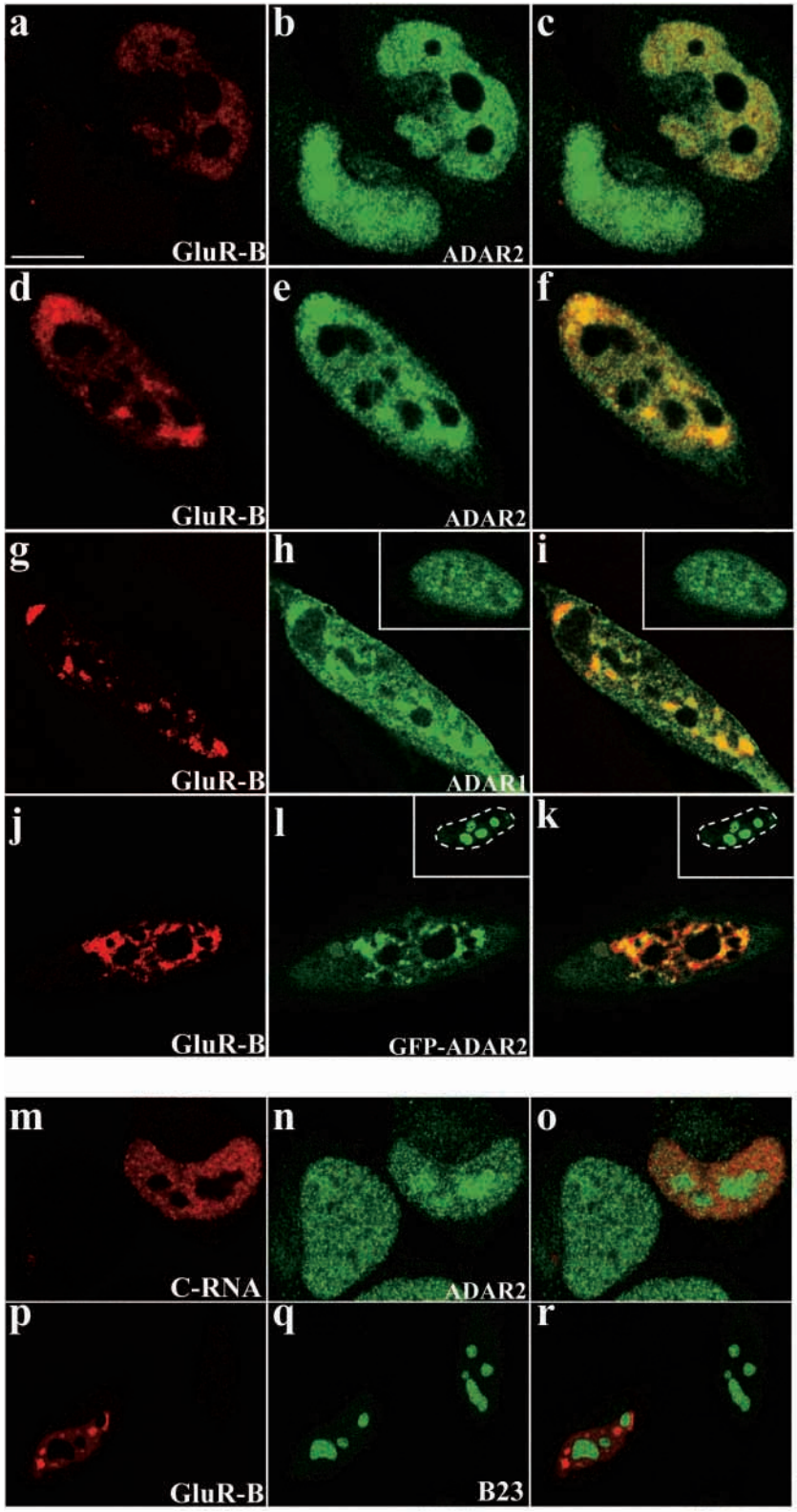

Fig. 9. Endogenous hADAR1 and hADAR2 are excluded from the nucleolus of cells expressing an editing substrate. HeLa cells were transiently transfected with a plasmid containing either the editing-competent murine GluR-B gene portion (Minigene B13) or a control gene portion from the Friends virus genome (C-RNA). Endogenous localization of editing enzymes was monitored by indirect immunofluorescence microscopy with antibodies directed against ADAR2 (b,e,n) and ADAR1 (Ab 668) (h). Alternatively, cells were transfected with a plasmid encoding GFP-ADAR2 (l). GluR-B- and C-RNA-transcribing cells were visualized by fluorescent in situ hybridization with a GluR-B (a,d,g,j,p) or C-RNA (m) probe labeled with digoxigenin. The hybridization sites were detected using a cy3 anti-digoxigenin secondary antibody. The GluR-B and C-RNA transcripts were detected ~40 hours after transfection. The GluR-B probe produces mainly a nucleoplasmic staining pattern, with nucleolar exclusion (a,d,g,j,p). In addition, transcripts tend to accumulate in discrete nucleoplasmic regions (d,g,j,p). In GluR-B-transcribing cells, ADAR2 and ADAR1 become completely excluded from the nucleolus (b,e,h,l). For comparison, cells that do not express GluR-B are shown in b (left side), h (inset) and l (inset). (e,h,l) Recruitment of ADAR1 and ADAR2 to the nucleoplasmic regions where GluR-B transcripts accumulate. In contrast to cells expressing GluR-B, ADAR2 persists concentrated in the nucleolus of cells expressing C-RNA (m-o). Furthermore, in contrast to ADAR1 and ADAR2, the nucleolar protein B23 remains in the nucleolus of cells expressing GluR-B transcripts (p-r). (c,f,i,k,o,r) A superimposition of the corresponding double-labeled images. Bar, 10 μm.

(amino acids 1-139) and two putative NLSs in the C-terminus (Fig. 7A). To try to identify the signal responsible for the observed nuclear and nucleolar localization, we produced deletion variants of hADAR2 fused to GFP at the N-terminus (Fig. 7A). The truncated versions of the protein were transiently transfected in HeLa cells and the localization analysed by confocal microscopy (Fig. 7B). HeLa cell extracts transfected with the different deletions were analysed by western blotting with an anti-GFP antibody and protein bands of the expected molecular mass were detected (data not

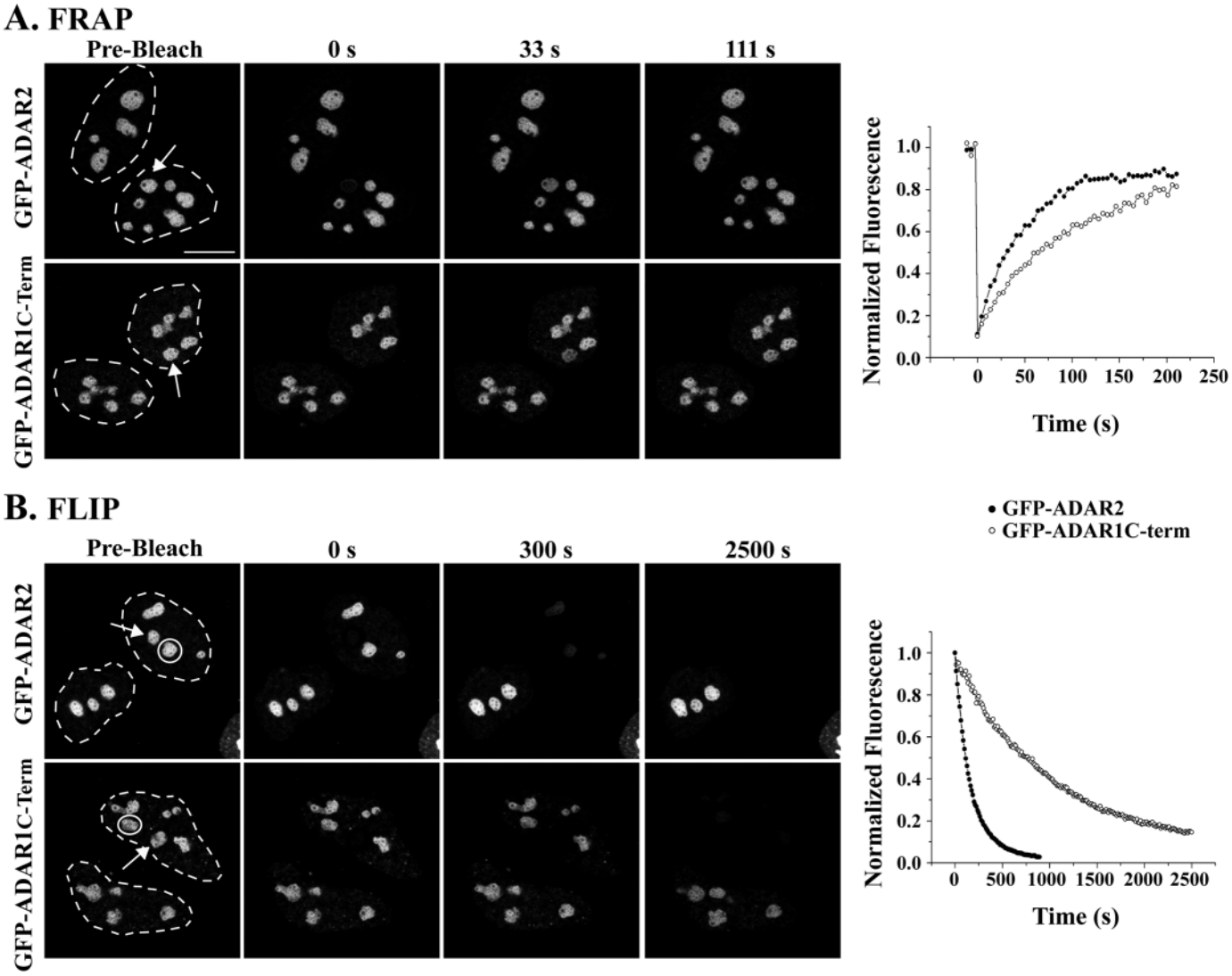

Fig. 10. FRAP and FLIP analysis of GFP-ADAR2 and GFP-ADAR1C-Term. (A) HeLa cells expressing either GFP-ADAR2 or GFP-ADAR1C-Term were bleached in a selected nucleolus for 0.5 seconds. Images were taken before bleaching and at the indicated time points after the end of the bleach pulse. (B) HeLa cells expressing either GFP-ADAR2 or GFP-ADAR1C-Term were repeatedly bleached in a selected nucleolus at intervals of 4.5 seconds. Images were taken before bleaching and at the indicated time points after the end of the first bleach pulse. The bleached nucleolus is indicated by an arrow in the pre-bleached panels. The dashed lines indicate the contour of the HeLa cell nucleus. Corresponding quantitative data of fluorescence-recovery kinetics are plotted on the right-hand side of each set of images. For FRAP experiments (A), the fluorescence intensity in the bleached region was measured and expressed as a relative fluorescence recovery (normalized fluorescence; see Materials and Methods). For FLIP experiments (B), the fluorescence intensity was measured in an adjacent nucleolus (marked by a white circle) and normalized as in FRAP experiments. Bar, 10 μm.

shown). GFP-ΔN localizes almost exclusively to the cytoplasm, whereas GFP fused to the first N-terminal 139 amino acids is primarily nuclear. This strongly suggests the presence of an active NLS in the N-terminal region, but only if the protein is devoid of an NES. Otherwise the cytoplasmic localization could be the result of a dominant export activity, as observed for full-length ADAR1 (Fig. 3A,B). To address this question, we treated the transfected cells with LMB (data not shown). After 5 hours of LMB treatment, the distribution of GFP-ΔN remained cytoplasmic, excluding the presence of a CRM1-dependent NES. Furthermore, ADAR2 remains restricted to the HeLa nucleus in an interspecies heterokaryon (Fig. 7C), indicating that the protein is devoid of any type of NES.

Surprisingly, deletion of a putative N-terminal NLS or stretches of basic amino acids (Δ64-75 and Δ64-132) had no effect on the nuclear accumulation of the protein, suggesting that hADAR2 contains a non-canonical NLS. Deletion of amino acid residues 64-75 (GFPΔ64-75) does not affect nucleolar localization, whereas deletion of residues 64-132 (GFPΔ64-132), which removes the first dsRBD, results in a protein that, although nuclear, is no longer able to concentrate in the nucleolus. Thus, the region between residues 75 and 132 is required for nucleolar targeting. Nevertheless, this stretch of

amino acids is not sufficient to target a GFP fusion to the nucleolus (see GFP-N1), suggesting that the correct localization of ADAR2 involves either a bipartite signal or a signal that is contiguous with sequences beyond amino acid 132.

In summary, the data show that ADAR2 is devoid of any NES, contains a non-canonical NLS within the first 64 amino acid residues and harbors a region between residues 75 and 132 that is necessary but not sufficient for nucleolar targeting.

Human cells express a third type of editing enzyme, hADAT, which shares homology with the C-terminus of hADAR1 and hADAR2 but lacks dsRBDs (Fig. 8). Unlike ADAR1 and ADAR2, which modify adenosines present in dsRNA and pre-mRNA, ADAT acts on tRNA (Maas et al., 1999). To analyse the cellular distribution of hADAT1, we fused GFP to the N-terminus of hADAT1. This chimera is detected in the nucleoplasm, with no nucleolar accumulation (Fig. 8). Thus, in contrast to hADAR1 and hADAR2, hADAT1 lacks a nucleolar targeting sequence. To investigate whether hADAT1 is permanently retained in the nucleus or shuttles between the nucleus and the cytoplasm, we made use of heterokaryons produced by fusion of HeLa cells transfected with GFP-ADAT1 and murine 3T3 cells (Fig. 8). The results show that GFP-ADAT1 molecules migrate from the transfected HeLa nucleus to the murine nuclei, implying that they are exported from the nucleus to the cytoplasm. Given the size of GFP-ADAT1 (82 kDa), this could be result of passive leakage through the pores. To distinguish between receptor-mediated transport and passive diffusion, HeLa cells expressing GFP-ADAT1 were transferred to 4°C in the presence of a protein-synthesis inhibitor. Receptor-mediated nuclear import and export are energy-dependent processes that are blocked at low temperature, whereas diffusion is unaffected (Michael et al., 1995). GFP-ADAT1 remains exclusively localized in the nucleus of HeLa cells incubated at 4°C (Fig. 8), indicating that GFP-ADAT1 does not diffuse passively to the cytoplasm. This suggests that, like hADAR1, hADAT1 shuttles across the nuclear pores, making use of a receptor-mediated export pathway. However, in striking contrast to hADAR1 and hADAR2, hADAT1 does not accumulate in the nucleolus.

Expression of an editing substrate delocalizes endogenous ADAR1 and ADAR2 from the nucleolus

To investigate whether the nucleolus represents a major editing site in the nucleus, we next examined the subcellular localization of an RNA that is known to be edited by both hADAR1 and hADAR2 (Dabiri et al., 1996; Hurst et al., 1995). HeLa cells were transiently transfected with a plasmid containing the editing-competent murine glutamate receptor GluR-B gene portion (B13 Minigene), which comprises both the Q/R site that is edited by ADAR2 and the hotspot-1 site in the intron that is edited by ADAR1 (Higuchi et al., 1993). Both enzymes are very specific and do not compete for editing a particular site. Fluorescent in situ hybridization using a GluR-B probe shows that GluR-B transcripts are present mainly in the nucleus. Within the nucleus, the GluR-B transcripts are non-homogeneously distributed in the nucleoplasm with clear nucleolar exclusion (Fig. 9a,d,g,j,p, red). Double-labeling experiments using anti-ADAR2 (Ab 70) and anti-ADAR1 (Ab 668) antibodies show that, in cells expressing the editing substrate, both enzymes become excluded from the nucleolus and co-localize precisely with the GluR-B transcripts in the nucleoplasm (Fig. 9b,e,h, green). Similar results were obtained with exogenously expressed GFP-ADAR2 and GFP-ADAR1C-Term (Fig. 9l, green, and data not shown). De-localization of ADAR1 and ADAR2 from the nucleolus was not observed in cells expressing transcripts from a plasmid that contains part of the Friend virus genome (Fig. 9m-o and data not shown). Recruitment of ADAR1 and ADAR2 from the nucleolus to the nucleoplasm of cells expressing GluR-B was further shown to be specific for editing enzymes, because the distribution of nucleolar components such as the protein B23 remains unaffected (Fig. 9p-r).

Taken together these results suggest that, although ADAR1 and ADAR2 localize to the nucleolus, editing substrates do not appear to be recruited there in order to be edited. Rather, the editing enzymes become excluded from the nucleolus when substrate pre-mRNAs are transcribed in the nucleoplasm. This suggests that the localization of ADAR1 and ADAR2 in the nucleolus is transient and most likely dynamic.

To examine the dynamic association of ADAR enzymes with the nucleolus in the living cell nucleus, we performed photobleaching experiments (FRAP and FLIP) using HeLa cells transfected with either GFP-ADAR2 or GFP-ADAR1C-Term. The vast majority of transfected HeLa cells contain several GFP-labeled nucleoli per nucleus. Using a high-powered spot laser pulse, the entire fluorescence associated with one nucleolus was bleached irreversibly. Then, in FRAP experiments the recovery of fluorescence signal in the bleached nucleolus was recorded by time-lapse imaging (Fig. 10A). The results show that the fluorescence produced by GFP-ADAR2 and GFP-ADAR1C-Term recovers within a few minutes after the bleach, indicating that unbleached GFP-fusion molecules have moved from the nucleoplasm into the bleached nucleolus. Because little fluorescence is visible in the nucleoplasm of these cells, it is most likely that the GFP-fusion molecules are in dynamic equilibrium between unbleached nucleoli and nucleoplasm. To confirm this result, FLIP experiments were performed (Fig. 10B). Bleaching over time of a single nucleolus eliminated the fluorescence in the other nucleoli, indicating that all fluorescent GFP-ADAR2 and GFP-ADAR1C-Term must be exchanging between the different nucleoli through the nucleoplasm. The results observed in FLIP are consistent with the FRAP experiments, showing a faster dynamics of GFP-ADAR2 compared with GFP-ADAR1C-Term. Overall, the data from photobleaching experiments suggest that in the living cell, ADAR1 and ADAR2 are constantly shuttling in and out of the nucleolus.

Discussion

In the present work, we have studied the subcellular localization of ADAR1 and ADAR2, the editing enzymes that deaminate adenosine to inosine in long dsRNA duplexes and specific pre-mRNA transcripts. Immunofluorescence analysis revealed that endogenous ADAR2 localizes to the nucleus and nucleolus, whereas ADAR1 distributes throughout the cytoplasm, nucleoplasm and nucleolus.

Several lines of evidence indicate the presence of short and long forms of ADAR1 in human cells. The long form of hADAR1 (150 kDa) localizes to the cytoplasm, is induced by

interferon and is thought to play a role in antiviral response mechanisms (Scadden and Smith, 2001). The shorter form (110 kDa) is exclusively nuclear because it lacks an NES present in the N-terminus of the full-length protein (Poulsen et al., 2001). Both forms are enzymatically active and it has been previously proposed that the nuclear 110 kDa version of hADAR1 represents a proteolytic cleavage fragment of the full-length protein (Patterson and Samuel, 1995). However, the data presented here argue that a mechanism of alternative usage of starting methionines can also occur in cells. Our data further show that both forms of hADAR1 accumulate in the nucleolus. The shorter form (110 kDa) localizes constitutively to the nucleolus (Fig. 2B), whereas the full-length form can only be detected in this compartment after inhibition of nuclear export (Fig. 3B).

Within the nucleolus, both ADAR2 and ADAR1C-Term are excluded from the fibrillar centers, the dense fibrillar component and the granular component. This represents the first evidence that editing enzymes occupy a novel subnucleolar compartment, raising the question of whether the nucleolus contains specific sites dedicated to RNA editing.

Although some nucleolar localization signals have been identified in proteins such HIV Tat and rev, mdm2, coilin, and ING1, it is currently accepted that there are no conserved nucleolar localization signals shared between nucleolar proteins (Andersen et al., 2002; Lyon and Lamond, 2000). One possibility is that proteins are not specifically targeted to the nucleolus but are instead retained within this compartment as a consequence of interactions with nucleolar components. Because the nucleolus is highly enriched in small nucleolar RNAs (snoRNAs) that form dsRNA structures with specific substrate rRNAs, and in small nuclear RNAs, it is conceivable that ADAR1 and ADAR2 localize to the nucleolus because they bind to these abundant dsRNAs. Consistent with this view, hADAT1 (which lacks dsRBDs) and the ADAR2 Δ64-132 mutant (which lacks the first dsRBD) do not accumulate in the nucleolus (Fig. 6B, Fig. 8).

Only a few physiological substrates for editing by ADAR1 and ADAR2 are known to date, and none has been localized to the nucleolus. Because the A-to-I RNA-editing mechanism requires a crucial dsRNA structure formed around editing sites (Smith et al., 1997), it is possible that some snoRNAs are potential substrates for editing. In this context, it is worth noting that a brain-specific snoRNA (mouse MBII-52 and its human ortholog HBII-52) has been identified that contains a guide region with an 18-nucleotide phylogenetically conserved complementarity to the serotonin receptor 5-HT_{2C} mRNA in a region containing two out of the four sites of adenosine-to-inosine editing within the serotonin receptor mRNA (Burns et al., 1997; Cavaille et al., 2000). Based on this finding, one could speculate that specific pre-mRNA substrates are targeted to the nucleolus in order to be edited, a view supported by the observation that some pre-mRNAs might transiently localize to the nucleolus before being exported to the cytoplasm (Bains et al., 1997; Bond and Wold, 1993; Pederson and Politz, 2000).

To test the hypothesis that pre-mRNA substrates are recruited to the nucleolus to be edited, we expressed the editing competent portion of glutamate receptor GluR-B pre-mRNA in HeLa cells (Higuchi et al., 1993). The results show that GluR-B transcripts accumulate in the nucleoplasm but are never detected in the nucleolus. Most importantly, both ADAR2 and ADAR1 become excluded from the nucleolus and accumulate at nucleoplasmic sites containing GluR-B transcripts. Thus, it appears that editing enzymes leave the nucleolus and are recruited to pre-mRNA substrates present in the nucleoplasm. Consistent with this view, we observe by photobleaching that ADAR1 and ADAR2 are constantly moving in and out of the nucleolus in the living cell.

In conclusion, the data suggest that, in living cells, editing might be regulated by the intracellular compartmentalization of editing enzymes. ADAR2 shuttles between the nucleolus and the nucleoplasm, whereas ADAR1 shuttles between the nucleolus, the nucleoplasm and the cytoplasm. During this flux, the enzymes might alternatively be recruited onto specific editing substrates present either in the nucleoplasm or in the cytoplasm, or be sequestered in the nucleolus.

We gratefully acknowledge Walter Keller (Biozentrum Basel, Switzerland) for kindly providing anti-ADAR1 and anti-ADAR2 antibodies, and Peter Seeburg (Max Planck Institute, Heidelberg) for the GluR-B/pRK plasmid. We are also grateful to our colleagues José Braga and José Rino for help with photobleaching experiments. We further thank Inês Condado, Maria do Carmo Silva and Helena Pina for technical support. This study was supported by grants from Fundação para a Ciência e Tecnologia, Portugal, and the European Commission (QLG2-CT-2001-01554). This work was also supported by the MRC, a grant from the British Heart Foundation (PG/98086), Ministerio de Ciencia y Tecnologia of Spain (BFI2002-00454) and Fundación Marqués de Valdecilla' of Santander, Spain (A05/02). J.M.P.D. was supported by a long-term fellowship of the European Molecular Biology Organization (EMBO-ALTF 239-2000).

References

Andersen, J. S., Lyon, C. E., Fox, A. H., Leung, A. K., Lam, Y. W., Steen, H., Mann, M. and Lamond, A. I. (2002). Directed proteomic analysis of the human nucleolus. *Curr. Biol.* **12**, 1-11.

Bains, M. A., Giles, I. and Wright, D. H. (1997). Distribution and configuration of c-*myc* RNA during transcriptional attenuation in differentiating cells in-situ. *Histochem. Cell. Biol.* **107**, 259-263.

Basilio, C., Wahba, A. J., Lengyel, P., Speyer, J. F. and Ochoa, S. (1962). Synthetic polynucleotides and the amino acid code. *Proc. Natl. Acad. Sci. USA* **48**, 613-616.

Bond, V. C. and Wold, B. (1993). Nucleolar localization of *myc* transcripts. *Mol. Cell. Biol.* **13**, 3221-3230.

Burd, C. G. and Dreyfuss, G. (1994). RNA binding specificity of hnRNP A1: significance of hnRNP A1 high-affinity binding sites in pre-mRNA splicing. *EMBO J.* **13**, 1197-1204.

Burns, C. M., Chu, H., Rueter, S. M., Hutchinson, L. K., Canton, H., Sanders-Bush, E. and Emeson, R. B. (1997). Regulation of serotonin-2C receptor G-protein coupling by RNA editing. *Nature* **387**, 303-308.

Calado, A., Kutay, U., Kuhn, U., Wahle, E. and Carmo-Fonseca, M. (2000). Deciphering the cellular pathway for transport of poly(A)-binding protein II. *RNA* **6**, 245-256.

Cavaille, J., Buiting, K., Kiefmann, M., Lalande, M., Brannan, C. I., Horsthemke, B., Bachellerie, J. P., Brosius, J. and Huttenhofer, A. (2000). Identification of brain-specific and imprinted small nucleolar RNA genes exhibiting an unusual genomic organization. *Proc. Natl. Acad. Sci. USA* **97**, 14311-14316.

Chen, C. X., Cho, D. S., Wang, Q., Lai, F., Carter, K. C. and Nishikura, K. (2000). A third member of the RNA-specific adenosine deaminase gene family, ADAR3, contains both single- and double-stranded RNA binding domains. *RNA* **6**, 755-767.

Choi, Y. D. and Dreyfuss, G. (1984). Monoclonal antibody characterization of the C proteins of heterogeneous nuclear ribonucleoprotein complexes in vertebrate cells. *J. Cell Biol.* **99**, 1997-2004.

Dabiri, G. A., Lai, F., Drakas, R. A. and Nishikura, K. (1996). Editing of the GLuR-B ion channel RNA in vitro by recombinant double- stranded RNA adenosine deaminase. *EMBO J.* **15**, 34-45.

Eckmann, C. R., Neunteufl, A., Pfaffstetter, L. and Jantsch, M. F. (2001).

The human but not the *Xenopus* RNA-editing enzyme ADAR1 has an atypical nuclear localization signal and displays the characteristics of a shuttling protein. *Mol. Biol. Cell* **12**, 1911-1924.

Gama-Carvalho, M., Krauss, R. D., Chiang, L., Valcarcel, J., Green, M. R. and Carmo-Fonseca, M. (1997). Targeting of U2AF65 to sites of active splicing in the nucleus. *J. Cell Biol.* **137**, 975-987.

George, C. X. and Samuel, C. E. (1999a). Characterization of the 5′-flanking region of the human RNA-specific adenosine deaminase *ADAR1* gene and identification of an interferon-inducible *ADAR1* promoter. *Gene* **229**, 203-213.

George, C. X. and Samuel, C. E. (1999b). Human RNA-specific adenosine deaminase ADAR1 transcripts possess alternative exon 1 structures that initiate from different promoters, one constitutively active and the other interferon inducible. *Proc. Natl. Acad. Sci. USA* **96**, 4621-4626.

Gerber, A. P. and Keller, W. (1999). An adenosine deaminase that generates inosine at the wobble position of tRNAs. *Science* **286**, 1146-1149.

Gerber, A. P. and Keller, W. (2001). RNA editing by base deamination: more enzymes, more targets, new mysteries. *Trends Biochem. Sci.* **26**, 376-384.

Gerber, A., O'Connell, M. A. and Keller, W. (1997). Two forms of human double-stranded RNA-specific editase 1 (hRED1) generated by the insertion of an Alu cassette. *RNA* **3**, 453-463.

Gerber, A., Grosjean, H., Melcher, T. and Keller, W. (1998). Tad1p, a yeast tRNA-specific adenosine deaminase, is related to the mammalian pre-mRNA editing enzymes ADAR1 and ADAR2. *EMBO J.* **17**, 4780-4789.

Gott, J. M. and Emeson, R. B. (2000). Functions and mechanisms of RNA editing. *Annu. Rev. Genet.* **34**, 499-531.

Higuchi, M., Single, F. N., Kohler, M., Sommer, B., Sprengel, R. and Seeburg, P. H. (1993). RNA editing of AMPA receptor subunit GluR-B: a base-paired intron-exon structure determines position and efficiency. *Cell* **75**, 1361-1370.

Higuchi, M., Maas, S., Single, F. N., Hartner, J., Rozov, A., Burnashev, N., Feldmeyer, D., Sprengel, R. and Seeburg, P. H. (2000). Point mutation in an AMPA receptor gene rescues lethality in mice deficient in the RNA-editing enzyme ADAR2. *Nature* **406**, 78-81.

Hough, R. F. and Bass, B. L. (2001). Adenosines deaminases that act on RNA. In *RNA Editing: Frontiers in Molecular Biology* (ed. B. L. Bass), pp. 77-108. Oxford University Press.

Hurst, S. R., Hough, R. F., Aruscavage, P. J. and Bass, B. L. (1995). Deamination of mammalian glutamate receptor RNA by *Xenopus* dsRNA adenosine deaminase: similarities to in vivo RNA editing. *RNA* **1**, 1051-1060.

Kawakubo, K. and Samuel, C. E. (2000). Human RNA-specific adenosine deaminase (*ADAR1*) gene specifies transcripts that initiate from a constitutively active alternative promoter. *Gene* **258**, 165-172.

Keegan, L. P., Gerber, A. P., Brindle, J., Leemans, R., Gallo, A., Keller, W. and O'Connell, M. A. (2000). The properties of a tRNA-specific adenosine deaminase from *Drosophila melanogaster* support an evolutionary link between pre-mRNA editing and tRNA modification. *Mol. Cell. Biol.* **20**, 825-833.

Keegan, L. P., Gallo, A. and O'Connell, M. A. (2001). The many roles of an RNA editor. *Nat. Rev. Genet.* **2**, 869-878.

Keller, W., Wolf, J. and Gerber, A. (1999). Editing of messenger RNA precursors and of tRNAs by adenosine to inosine conversion. *FEBS Lett.* **452**, 71-76.

Kumar, M. and Carmichael, G. G. (1997). Nuclear antisense RNA induces extensive adenosine modifications and nuclear retention of target transcripts. *Proc. Natl. Acad. Sci. USA* **94**, 3542-3547.

Lafarga, M., Berciano, M. T., Garcia-Segura, L. M., Andres, M. A. and Carmo-Fonseca, M. (1998). Acute osmotic/stress stimuli induce a transient decrease of transcriptional activity in the neurosecretory neurons of supraoptic nuclei. *J. Neurocytol.* **27**, 205-217.

Lichter, P., Boyle, A. L., Cremer, T. and Ward, D. C. (1991). Analysis of genes and chromosomes by nonisotopic in situ hybridization. *Genet. Anal. Tech. Appl.* **8**, 24-35.

Lyon, C. E. and Lamond, A. I. (2000). The nucleolus. *Curr. Biol.* **10**, R323.

Maas, S., Gerber, A. P. and Rich, A. (1999). Identification and characterization of a human tRNA-specific adenosine deaminase related to the ADAR family of pre-mRNA editing enzymes. *Proc. Natl. Acad. Sci. USA* **96**, 8895-8900.

Melcher, T., Maas, S., Herb, A., Sprengel, R., Seeburg, P. H. and Higuchi, M. (1996). A mammalian RNA editing enzyme. *Nature* **379**, 460-464.

Michael, W. M., Choi, M. and Dreyfuss, G. (1995). A nuclear export signal in hnRNP A1: a signal-mediated, temperature-dependent nuclear protein export pathway. *Cell* **83**, 415-422.

O'Connell, M. A., Krause, S., Higuchi, M., Hsuan, J. J., Totty, N. F., Jenny, A. and Keller, W. (1995). Cloning of cDNAs encoding mammalian double-stranded RNA-specific adenosine deaminase. *Mol. Cell. Biol.* **15**, 1389-1397.

O'Connell, M. A., Gerber, A. and Keller, W. (1997). Purification of human double-stranded RNA-specific editase 1 (hRED1) involved in editing of brain glutamate receptor B pre-mRNA. *J. Biol. Chem.* **272**, 473-478.

O'Connell, M. A., Gerber, A. and Keegan, L. P. (1998). Purification of native and recombinant double-stranded RNA-specific adenosine deaminases. *Methods* **15**, 51-62.

Palladino, M. J., Keegan, L. P., O'Connell, M. A. and Reenan, R. A. (2000). dADAR, a *Drosophila* double-stranded RNA-specific adenosine deaminase is highly developmentally regulated and is itself a target for RNA editing. *RNA* **6**, 1004-1018.

Patterson, J. B. and Samuel, C. E. (1995). Expression and regulation by interferon of a double-stranded-RNA-specific adenosine deaminase from human cells: evidence for two forms of the deaminase. *Mol. Cell. Biol.* **15**, 5376-5388.

Patton, D. E., Silva, T. and Bezanilla, F. (1997). RNA editing generates a diverse array of transcripts encoding squid Kv2 K^+ channels with altered functional properties. *Neuron* **19**, 711-722.

Pederson, T. and Politz, J. C. (2000). The nucleolus and the four ribonucleoproteins of translation. *J. Cell Biol.* **148**, 1091-1095.

Phair, R. D. and Misteli, T. (2000). High mobility of proteins in the mammalian cell nucleus. *Nature* **404**, 604-609.

Pinol-Roma, S. and Dreyfuss, G. (1992). Shuttling of pre-mRNA binding proteins between nucleus and cytoplasm. *Nature* **355**, 730-732.

Poulsen, H., Nilsson, J., Damgaard, C. K., Egebjerg, J. and Kjems, J. (2001). CRM1 mediates the export of ADAR1 through a nuclear export signal within the Z-DNA binding domain. *Mol. Cell. Biol.* **21**, 7862-7871.

Reimer, G., Pollard, K. M., Penning, C. A., Ochs, R. L., Lischwe, M. A., Busch, H. and Tan, E. M. (1987). Monoclonal autoantibody from a (New Zealand black × New Zealand white)F1 mouse and some human scleroderma sera target an Mr 34,000 nucleolar protein of the U3 RNP particle. *Arthritis Rheum.* **30**, 793-800.

Scadden, A. D. and Smith, C. W. (2001). Specific cleavage of hyper-edited dsRNAs. *EMBO J.* **20**, 4243-4252.

Singh, M. and Emeson, R. B. (2000). Adenosine-to-inosine RNA editing: substrates and consequences. In *RNA Editing: Frontiers in Molecular Biology* (ed. B. L. Bass), pp. 109-138. Oxford University Press.

Smith, H. C., Gott, J. M. and Hanson, M. R. (1997). A guide to RNA editing. *RNA* **3**, 1105-1123.

Sommer, B., Kohler, M., Sprengel, R. and Seeburg, P. H. (1991). RNA editing in brain controls a determinant of ion flow in glutamate-gated channels. *Cell* **67**, 11-19.

Taylor, J. M. (1990). Hepatitis delta virus: *cis* and *trans* functions required for replication. *Cell* **61**, 371-373.

Wang, Q., Khillan, J., Gadue, P. and Nishikura, K. (2000). Requirement of the RNA editing deaminase *ADAR1* gene for embryonic erythropoiesis. *Science* **290**, 1765-1768.

Zhang, Z. and Carmichael, G. G. (2001). The fate of dsRNA in the nucleus: a $p54^{nrb}$-containing complex mediates the nuclear retention of promiscuously A-to-I edited RNAs. *Cell* **106**, 465-475.